Electronic Supplementary Material (ESI) for Nanoscale

Supporting Information

Lattice dynamics in atomically thin sheets of WS_2 and WSe_2

Weijie Zhao[a,c,#], *Zohreh Ghorannevis*[a,c,#], *Amara Kiran Kumar*[b], *Jing Ren Pang*[b], *Minglin Toh*[d], *Xin Zhang*[e], *Christian Kloc*[d], *Ping Heng Tan*[e], *Goki Eda*[a,b,c,*]

[a] Department of Physics, National University of Singapore, 2 Science Drive 3, Singapore 117542

[b] Department of Chemistry, National University of Singapore, 3 Science Drive 3, Singapore 117543

[c] Graphene Research Centre, National University of Singapore, 6 Science Drive 2, Singapore 117546

[d] School of Materials Science and Engineering, Nanyang Technological University, N4.1 Nanyang Avenue, Singapore 639798

[e] State Key Laboratory of Superlattices and Microstructures, Institute of Semiconductors, Chinese Academy of Sciences, Beijing 100083, China

[*] E-mail: g.eda@nus.edu.sg

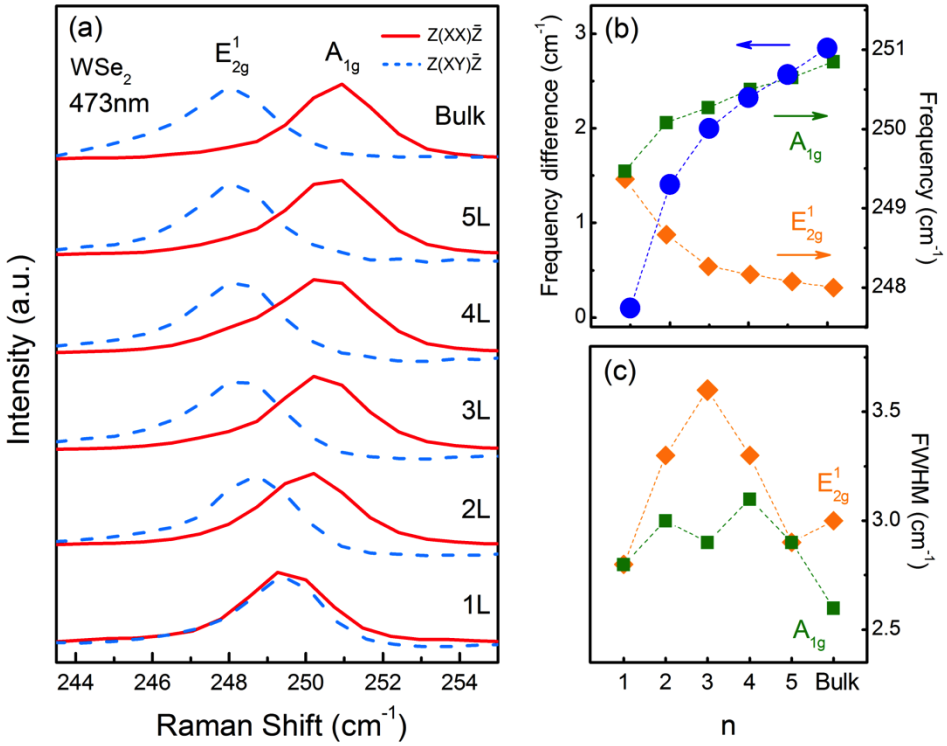

Figure S1 - (a) Raman spectra of 1 to 5L and bulk WSe_2 obtained in the parallel ($Z(XX)\bar{Z}$) and cross ($Z(XY)\bar{Z}$) polarization conditions obtained with 473 nm excitation. The spectra are normalized and vertically offset for clarity. (b) Position of the and modes (right vertical axis) and their difference (left vertical axis) as a function of the number of layers (n). (c) FWHM (right vertical axis) of A_{1g} and E^1_{2g} modes as a function of the number of layers.

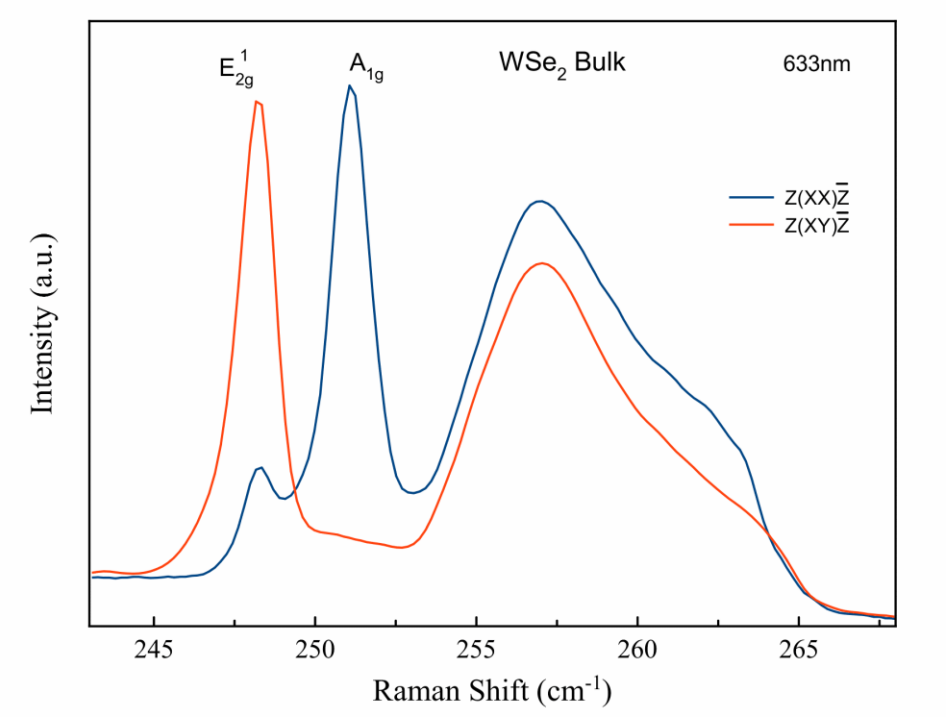

Figure S2 - Raman spectra of bulk WSe_2 obtained in the parallel ($Z(XX)\bar{Z}$) and cross ($Z(XY)\bar{Z}$) polarization conditions with 633 nm excitation. The spectra are normalized.

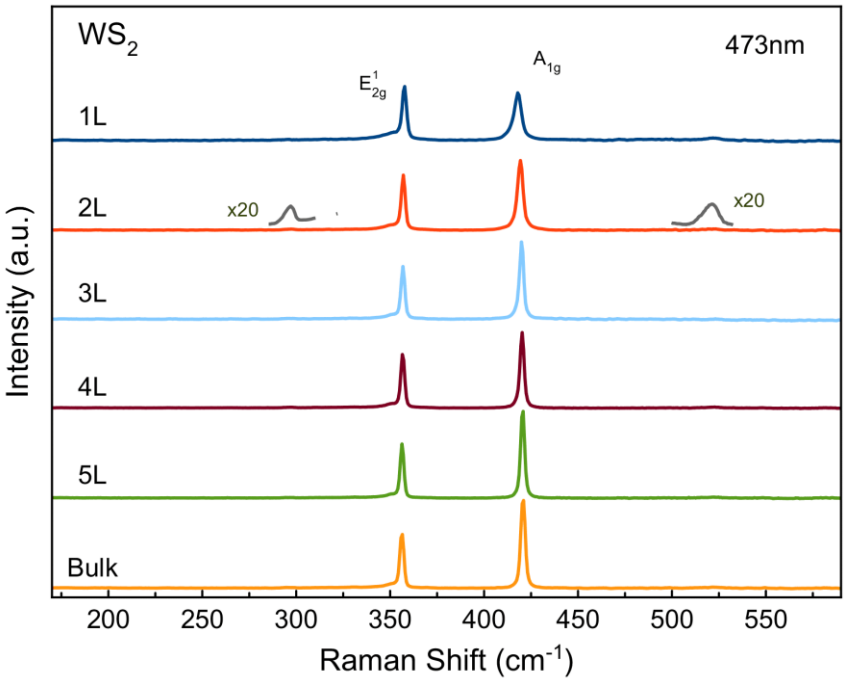

Figure S3 - Raman spectra of 1-5L and bulk WS_2 obtained by 473nm laser excitation.

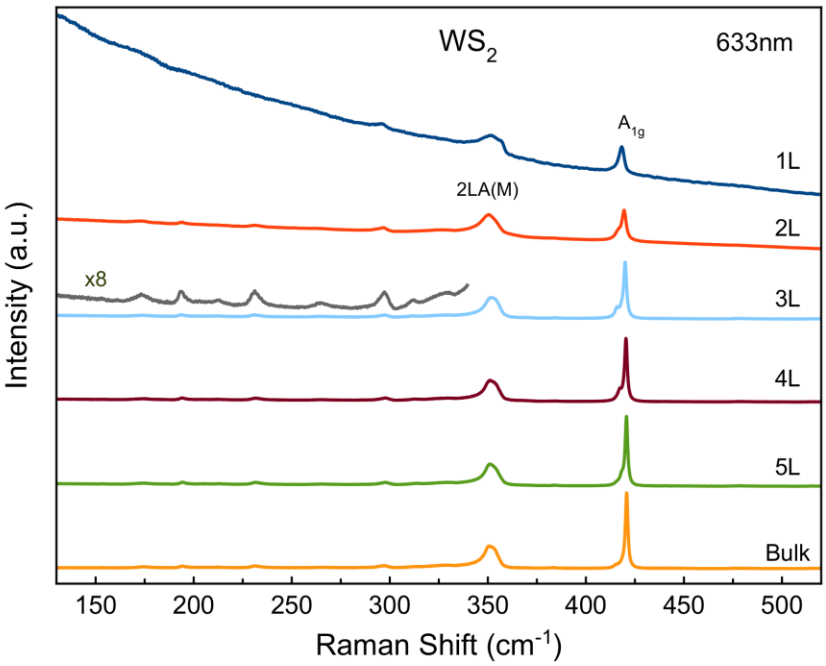

Figure S4 – Unpolarized Raman spectra of 1 to 5L and bulk WS_2 obtained with 633 nm laser excitation. Resonance features are observed in all spectra. Photoluminescence background is observed in monolayer WS_2 spectrum.

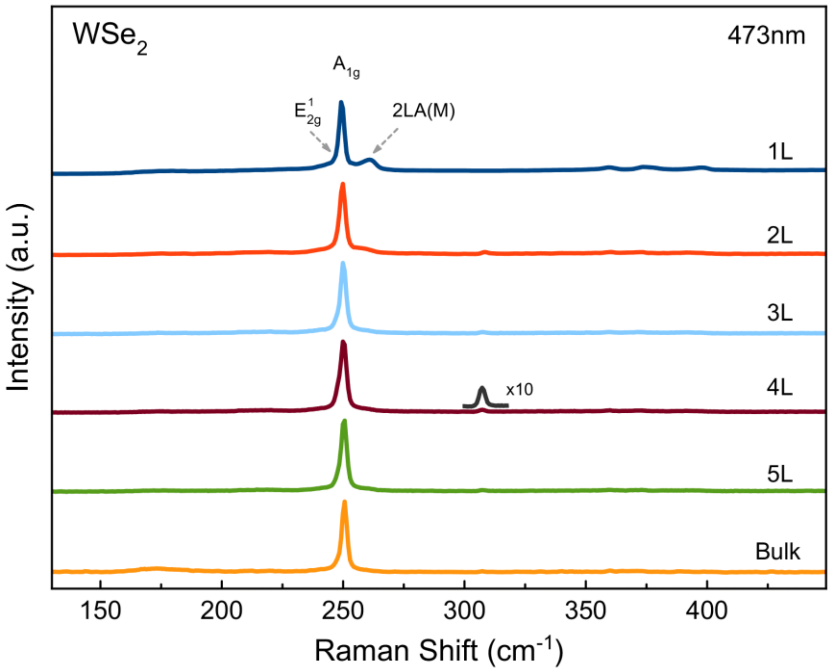

Figure S5 – Unpolarized Raman spectra of 1 to 5L and bulk WSe_2 obtained with 473 nm laser excitation. Some resonance Raman features are observed.

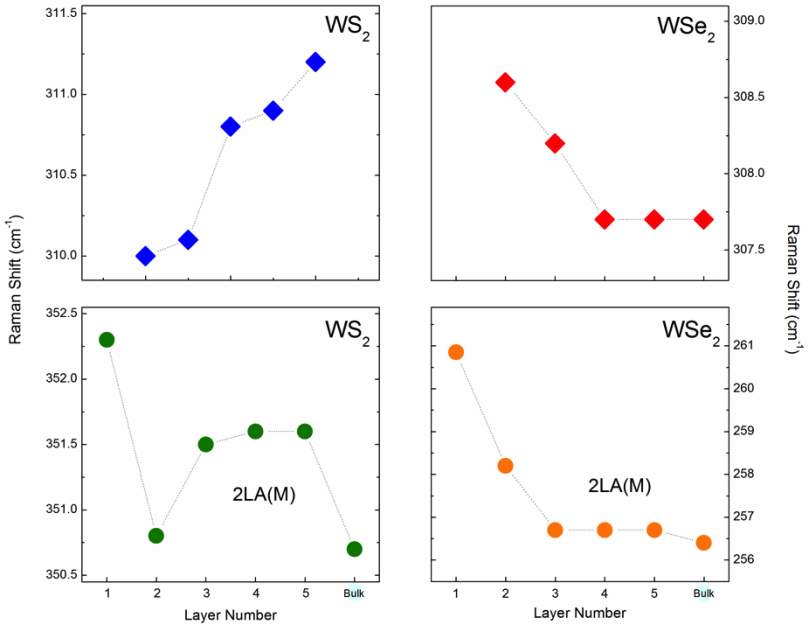

Figure S6 – Thickness dependence of some resonance Raman features observed with 532 nm laser excitation.

Table S1 - Tentative assignments of multiphonon bands observed in the resonance Raman spectra of WS_2 and WSe_2. “y” indicates that the mode is observed. “1L(no)” indicates that the mode is absent in monolayers but observed in multilayers.

Peak(cm^{-1})	473nm	532nm	633nm	Possible assignments
WS_2				
170		1L(no)		$E^1_{2g}(M)-LA(M)$
173		y	y	$E^1_{2g}(M)-LA(M)$
194		y	y	$B_{2g}(M)-LA(M)$
231		y	y	$A_{1g}(M)-LA(M)$
265		y	y	$A_{1g}(M)$-$ZA(M)$?
298	y	y	y	$2ZA(M)$?
311		1L(no)	y	?
326		y	y	$LA(M)+TA(M)$?
350	y	y	y	$2LA(M)$
522	y	y	y	$E^1_{2g}(M)+LA(M)$
WSe_2				
136		y	y	$A_{1g}(M)-LA(M)$
260	y	y	y	$2LA(M)$
308	1L(no)	1L(no)		?
360	y	y	y	$2E_{1g}(\Gamma)$ or $A_{1g}(M)+TA(M)$
373	y	y	y	$E^1_{2g}(M)+LA(M)$
394	y	y	y	$3LA(M)$?

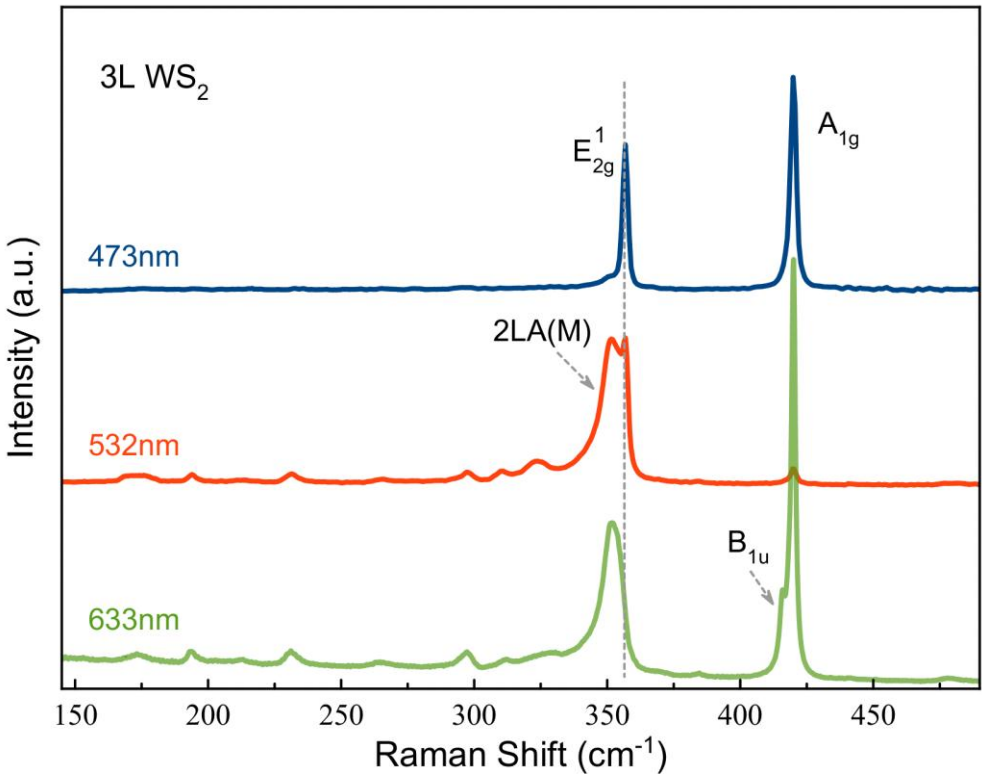

Figure S7 – Unpolarized Raman spectra of 3L WS_2 sample with 473, 532 and 633 nm laser excitations. The spectra are normalized by the E^1_{2g} peak for 473 and 532nm excitations and by the 2LA(M) mode for 633nm laser excitation. The vertical dashed line indicates the position of E^1_{2g} peak.

Figure S7 shows the unpolarized Raman spectra of a 3L WS_2 sample obtained using three excitation lasers (473, 532 and 633 nm). For 473 nm excitation, which matches in energy with the density of states absorption peak, 2LA(M) peak is observed as a small left shoulder of the E^1_{2g} peak. In contrast, the 2LA(M) peak is significantly enhanced with respect to the E^1_{2g} peak for 532 nm and 633 nm excitations, which are in resonance with the excitonic absorption peaks.

The E^1_{2g} and A_{1g} modes are both equally enhanced in the interband resonance for 473 nm laser excitation. In contrast, the A_{1g} peak is found to be significantly weak in intensity compared to the E^1_{2g} peak for 532 nm excitation. For the 633 nm laser

excitation, a reverse effect is observed where the A_{1g} peak is significantly more intense compared to the E^1_{2g} peak, which is buried in the 2LA(M) peak. This suggests that each Raman mode has different cross-section enhancement for a given excitation condition.

The A and B excitonic absorption in WS_2 mainly correspond to the transitions from the d_{xy} and $d_{x^2-y^2}$ states to d_{z^2} states of the tungsten atom [*S1, S2, S3*]. Thus, electrons excited by the 633 nm laser have a character of the tungsten d_{z^2} orbitals aligned along the c axis perpendicular to the WS_2 basal plane. Since the A_{1g} phonons involve atomic displacements along the c-axis [*S4, S5*], the A_{1g} phonons can couple more strongly with the excited d_{z^2} states than with the E^1_{2g} phonons. Consequently, the enhancement of the A_{1g} mode is much stronger than the E^1_{2g} mode at excitonic resonance for 633 nm laser. A similar effect has been observed in MoS_2 monolayers and nanoparticles [*S6, S7*]. On the other hand, the reverse effect observed for the 532 nm excitation cannot be explained by the same mechanism. This is likely due to electron-phonon coupling involving not only the d_{z^2} electrons but also other electrons from inter-band transitions [*S1, S2, S3*].

A peak at ~416 cm^{-1} observed with 633 nm excitation was previously assumed to be a combination of LA and TA phonons at the K point [*S8*]. However, recent theoretical studies of WS_2 phonon dispersion curves [*S9, S10*] suggest that this is B_{1u} mode at the Γ point. The B_{1u} mode is the Davydov doublet with the A_{1g} mode [*S4, S5, S11*]. Studies have shown that this mode is enhanced with increase in disorder in WS_2 nanotubes [*S12*]. This indicates that the B_{1u} mode may be used for monitoring defects in WS_2, sheets, similar to the D mode in graphene-based materials [*S13*], and deserves further investigation.

References:

S1. Coehoorn, R.; Haas, C.; de Groot, R. A., Electronic structure of MoSe2, MoS2, and WSe2. II. The nature of the optical band gaps. *Physical Review B* 1987**,** *35* (12), 6203-6206.

S2. Ramasubramaniam, A., Large excitonic effects in monolayers of molybdenum and tungsten dichalcogenides. Physical Review B 2012, 86 (11), 115409.

S3. Yun, W. S.; Han, S. W.; Hong, S. C.; Kim, I. G.; Lee, J. D., Thickness and strain effects on electronic structures of transition metal dichalcogenides: 2H-MX2 semiconductors (M = Mo, W; X = S, Se, Te). Physical Review B 2012, 85 (3), 033305.

S4. Wieting, T. J.; Verble, J. L., Infrared and Raman Studies of Long-Wavelength Optical Phonons in Hexagonal MoS2. Physical Review B 1971, 3 (12), 4286-4292.

S5. Sekine, T.; Nakashizu, T.; Toyoda, K.; Uchinokura, K.; Matsuura, E., Raman scattering in layered compound 2H-WS2. Solid State Communications 1980, 35 (4), 371-373.

S6. Chakraborty, B.; Bera, A.; Muthu, D. V. S.; Bhowmick, S.; Waghmare, U. V.; Sood, A. K., Symmetry-dependent phonon renormalization in monolayer MoS2 transistor. Physical Review B 2012, 85 (16), 161403.

S7. Frey, G. L.; Tenne, R.; Matthews, M. J.; Dresselhaus, M. S.; Dresselhaus, G., Raman and resonance Raman investigation of MoS2 nanoparticles. Physical Review B 1999, 60 (4), 2883-2892.

S8. Sourisseau, C.; Cruege, F.; Fouassier, M.; Alba, M., Second-order Raman effects, inelastic neutron scattering and lattice dynamics in 2H-WS2. Chemical Physics 1991, 150 (2), 281-293.

S9. Molina-Sanchez, A.; Wirtz, L., Phonons in single-layer and few-layer MoS2 and WS2. Physical Review B 2011, 84 (15).

S10. Ataca, C.; Şahin, H.; Ciraci, S., Stable, Single-Layer MX2 Transition-Metal Oxides and Dichalcogenides in a Honeycomb-Like Structure. The Journal of Physical Chemistry C 2012, 116 (16), 8983-8999.

S11. Ghosh, P. N.; Maiti, C. R., Interlayer force and Davydov splitting in 2H-MoS2. Physical Review B 1983, 28 (4), 2237-2239.

S12. Staiger, M.; Rafailov, P.; Gartsman, K.; Telg, H.; Krause, M.; Radovsky, G.; Zak, A.; Thomsen, C., Excitonic resonances in WS2 nanotubes. Physical Review B 2012, 86 (16), 165423.

S13. Ferrari, A. C., Raman spectroscopy of graphene and graphite: Disorder, electron–phonon coupling, doping and nonadiabatic effects. *Solid State Communications* **2007,** *143* (1–2), 47-57.